Bioorganic & Medicinal Chemistry 18 (2010) 4769–4774

Contents lists available at ScienceDirect

Bioorganic & Medicinal Chemistry

journal homepage: www.elsevier.com/locate/bmc

Crystallographic and docking studies of purine nucleoside phosphorylase from *Mycobacterium tuberculosis*

Rodrigo G. Ducati [a], Luiz A. Basso [a], Diógenes S. Santos [a,*], Walter F. de Azevedo Jr. [b,*]

[a] *Centro de Pesquisas em Biologia Molecular e Funcional, Instituto de Pesquisas Biomédicas, Pontifícia Universidade Católica do Rio Grande do Sul (PUCRS), Avenida Ipiranga 6681/92-A, 90619-900 Porto Alegre, RS, Brazil*

[b] *Faculdade de Biociências, Instituto Nacional de Ciência e Tecnologia em Tuberculose-CNPq, Laboratório de Bioquímica Estrutural (LaBioQuest), Pontifícia Universidade Católica do Rio Grande do Sul (PUCRS), Porto Alegre, RS, Brazil*

ARTICLE INFO

Article history:
Received 10 March 2010
Revised 1 May 2010
Accepted 4 May 2010
Available online 10 May 2010

Keywords:
Human tuberculosis
Purine nucleoside phosphorylase
2-Methyl-adenosine
Rational drug design
Polynomial empirical scoring function

ABSTRACT

This work describes for the first time the structure of purine nucleoside phosphorylase from *Mycobacterium tuberculosis* (MtPNP) in complex with sulfate and its natural substrate, 2′-deoxyguanosine, and its application to virtual screening. We report docking studies of a set of molecules against this structure. Application of polynomial empirical scoring function was able to rank docking solutions with good predicting power which opens the possibility to apply this new criterion to analyze docking solutions and screen small-molecule databases for new chemical entities to inhibit MtPNP.

1. Introduction

Epidemiological studies have indicated that 1.7 billion people, as much as one third of the world's population, are infected with *Mycobacterium tuberculosis*, the causative agent of human tuberculosis (TB). This pathogen is responsible for more human deaths than any other single infectious agent throughout the centuries of human history, accounting for 26% of all preventable deaths and 7% of all deaths.[1] It is estimated that approximately 95% of TB cases are distributed among developing nations, which account for 98% of the deaths worldwide,[2] mostly because these countries have both limited resources to ensure the proper treatment and high incidence of human immunodeficiency virus infection.[3,4]

The resurgence of TB as a global public health threat in developed countries has been attributed to various factors, the most worrisome being the widespread emergence of drug-resistance,[3,5] since it becomes more difficult and expensive to treat, and more likely to be fatal.[6,7] As no drugs have been developed for the last few decades to replace the ones *M. tuberculosis* has acquired resistance for,[8] and since bacille Calmette–Guérin vaccine cannot prevent reactivation of latent infection in adults,[9] new drugs and vaccines are needed to combat TB in a chemotherapeutic and prophylactic manner.[10]

The complete genome sequencing of *M. tuberculosis*[11] has given the scientific community a databank on which to explore singular features of this pathogen. Enzymes of metabolic pathways can be evaluated as possible targets for drug development.[12,13] The purine recycling and salvage pathways represent essential cellular processes that are critical for the life of many organisms.[14] *M. tuberculosis* purine metabolism has been implicated in bacterial latency.[15,16] Purine nucleoside phosphorylase (PNP; EC 2.4.2.1) plays a critical role in the phosphorolysis of purine nucleosides and deoxynucleosides to generate purine bases.[14] The enzyme from *M. tuberculosis* (MtPNP) is a member of the trimeric class, which includes the human (HsPNP) and bovine homologues, among others, a family of PNPs that differs significantly from the hexameric class usually present in bacteria.[17] Substrate specificities are considerably dissimilar among these classes, as a consequence of the substantial divergence of residue composition at the catalytic site.[18]

Even though PNP activity is shared between mammals and *M. tuberculosis*, drugs with selective toxicity against MtPNP can be

Abbreviations: TB, human tuberculosis; PNP, purine nucleoside phosphorylase; MtPNP, PNP from *Mycobacterium tuberculosis*; HsPNP, human PNP; 2dGuo, 2′-deoxyguanosine; VS, virtual screening; POLSCORE, polynomial empirical scoring function; MESG, 2-amino-6-mercapto-7-methylpurine ribonucleoside; RMSD, root mean square deviation; PLP, piecewise linear potential; DADME-IMMH, 7-[[(3*R*,4*R*)-3-hydroxy-4-(hydroxymethyl)pyrrolidin-1-yl]methyl]-1,5 dihydropyrrolo[3,2-d]pyrimidin-4-one; DMSO, dimethyl sulfoxide; HEPES, *N*-2-hydroxyethylpiperazine-*N*′-2-ethanesulfonic acid.

* Corresponding authors. Tel./fax: +55 51 33203629.
E-mail addresses: diogenes@pucrs.br (D.S. Santos), walter@azevedolab.net, wfdaj@uol.com.br (W.F. de Azevedo Jr.).

0968-0896/$ - see front matter © 2010 Elsevier Ltd. All rights reserved.
doi:10.1016/j.bmc.2010.05.009

developed based on the knowledge of their differences.[13,19] A number of research groups have dedicated their efforts to determine specificity of substrates, kinetic mechanisms, and three-dimensional structures for PNPs from different bacterial sources[18,20–26] in comparison with HsPNP. In the present work, efforts have been made to determine the crystallographic structure of MtPNP in complex with 2′-deoxyguanosine (2dGuo; Fig. 1), a natural substrate for PNPs, and sulfate ion. Furthermore, we employed purine nucleoside as a pharmacophore to build up a database of similar compounds and performed virtual screening (VS) focused on the MtPNP active site. The ligand with the highest affinity for the MtPNP active site is 2-methyl-adenosine, a molecule that has been previously shown to display antimycobacterial activity.[13,27,28] In addition, a polynomial empirical scoring function (POLSCORE)[29,30] was employed to estimate ligand-binding affinity and applied to rank docking results.

2. Results and discussion

2.1. Overall analysis of MtPNP:sulfate:2′-deoxyguanosine crystal structure

Parameters of data collection, refinement statistics, and structure quality are listed in Table 1. Since it has been verified that MtPNP requires the presence of inorganic phosphate in order to bind 2dGuo,[20] we used sulfate instead of phosphate to gather information on the crystal structure of an active form of the ternary complex with no enzyme-catalyzed chemical reaction. This same strategy has been previously reported using 2-amino-6-mercapto-7-methylpurine ribonucleoside (MESG), a nucleoside analogue.[31] In a simple assay at 258 nm, sulfate proved to have no capacity in kinetically replacing phosphate (data not shown). Accordingly, although MtPNP:sulfate:2dGuo represents an active form of a ternary complex, it cannot support chemical reaction.

2.2. Crystallographic structure of MtPNP:sulfate:2dGuo

All MtPNP crystallographic structures solved so far (PDB access codes: 1G2O, 1I80, 1N3I, and the present structure)[32,33] show differences between R_{free} and R_{factor} of approximately 7%. This difference may indicate intrinsic flexibility of these structures, represented experimentally by crystallographic *B* values observed in regions close to the active site and at N and C termini.

The structure of MtPNP:sulfate:2dGuo follows the same fold as other PNPs.[26,32,33] The crystallography data revealed that the structure is a dimer in the asymmetric unit although the canonical trimer can be built from the symmetry relationship. Figures 2 and 3 show the crystal packing and the crystallographic trimer, respectively. Each monomer displays an alpha/beta fold consisting of a mixed beta-sheet surrounded by alpha-helices. The analysis of the electron density maps at the final stages of the crystallographic refinement shows that the ligand (2dGuo) is, not surprisingly, in the binding site of PNP (Fig. 4) and is anchored by the two main residues of the binding pocket (Glu 189 and Asn 231).

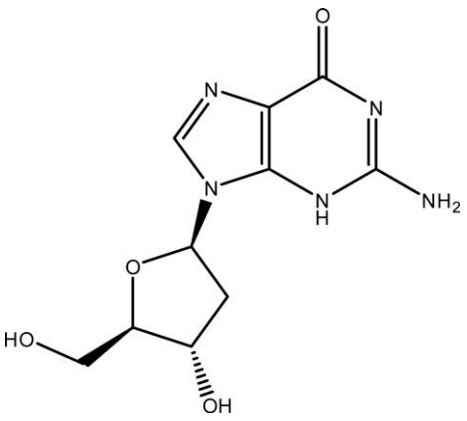

Figure 1. Structure of 2′-deoxyguanosine.

Table 1
Data collection and refinement statistics

Cell parameters	
$a = b$ (Å)	113.48
c (Å)	85.01
Space group	*H*3
Number of measurements with $I > 2\sigma(I)$	145364
Number of independent reflections	21219
Completeness of data (%)	96.9
R_{sym}[a] (%)	8.6
Highest resolution shell (Å)	2.27–2.15
Completeness in highest resolution shell (%)	81.8
R_{sym}[a] in the highest resolution shell (%)	13.8
Resolution range used in the refinement (Å)	28.34–2.15
R_{factor}[b] (%)	17.5
R_{free}[c] (%)	24.9
Observed RMSD from ideal geometry	
Bond length (Å)	0.022
Bond angles (°)	1.976
B values[d] *(Å²)*	
Main chain	17.21
Side chains	18.61
2′-Deoxyguanosine	22.39
Waters	23.52
Sulfate groups	23.17
Residues in the most favored regions of Ramachandran plot (%)	90.2
Residues in additionally allowed regions of Ramachandran plot (%)	8.6
Residues in generously allowed regions of Ramachandran plot (%)	0.5
Residues in the disallowed regions of Ramachandran plot (%)	0.7
Number of water molecules	209
Number of sulfate molecules	2

[a] $R_{sym} = 100\Sigma|I(h) - \langle I(h)\rangle|/\Sigma I(h)$ with $I(h)$, observed intensity and $\langle I(h)\rangle$, mean intensity of reflection h over all measurements of $I(h)$.
[b] $R_{factor} = 100\Sigma|F_{obs} - F_{calc}|/\Sigma(F_{obs})$, the sums being taken over all reflections with $F/(F) > 2$ cuttoff.
[c] $R_{free} = R_{factor}$ for 10% of the data, which were not included during crystallographic refinement.
[d] *B* values = average *B* values for all non-hydrogen atoms.

The specificity and affinity between an enzyme and a ligand depend on directional hydrogen bonds and ionic interactions, as well as on the shape complementarity of the contact surfaces of both partners.[34,35] The interaction of the ligand and MtPNP was evaluated with the program MOLDOCK, which revealed six hydrogen bonds between the ligand and the residues Ser 35, Glu 189, Asn 231, and His 243, and hydrophobic contacts with other residues of the binding pocket (Ala 120, Tyr 188, Val 205, Met 207, and Val 246).

2.3. Docking simulations

The use of the MOLDOCK[36,37] to the structure of MtPNP in complex with 2dGuo was capable of correctly predicting its positioning in the binding pocket of MtPNP. Figure 5A shows the superposition of the best docked structure and crystallographic structure, the root mean square deviation (RMSD) of superposition of non-hydrogen atoms is 0.7 Å. In addition, we applied the same docking protocol to three previously solved structures of MtPNPs (PDB access codes: 1G2O, 1I80, and 1N3I) deposited in the PDB, which generated RMSD from 0.2 to 0.4 Å. These altogether, strongly indicated that the present docking protocol can be employed against any

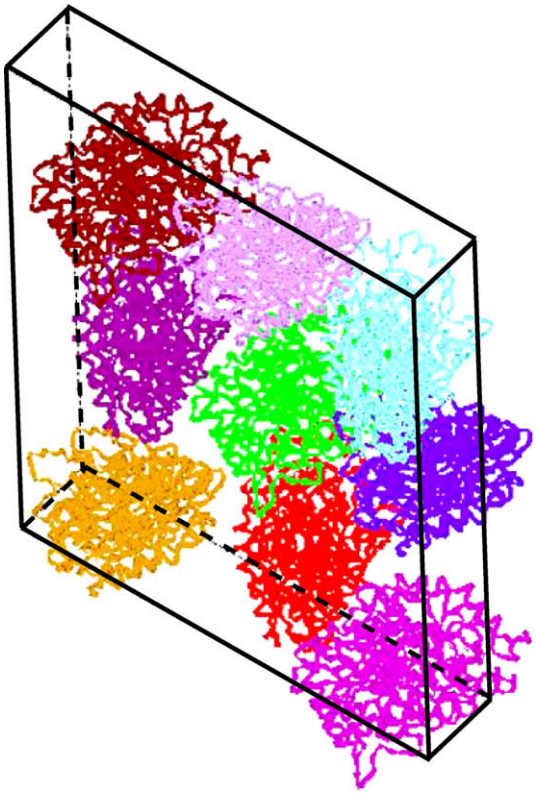

Figure 2. Crystal packing for the MtPNP:sulfate:2dGuo complex.

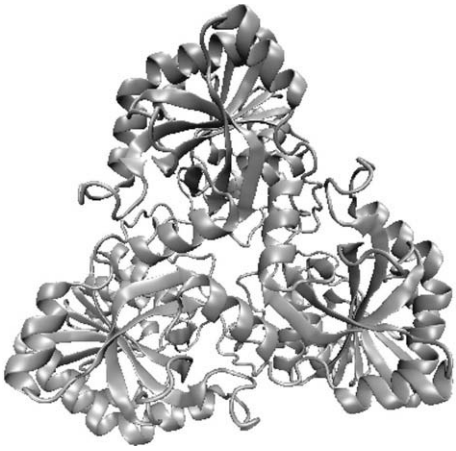

Figure 3. Trimeric structure for the MtPNP:sulfate:2dGuo complex.

of these MtPNP structures (Fig. 5B–D). Since this docking protocol seems capable of reproducing the crystallographic structure, we applied it to a data set of molecules having a purine nucleoside core in their structures.

Furthermore, in order to carry out a set of cross-docking simulations for MtPNP, all ligands taken from the crystal structures of the MtPNP were docked onto a selected structure (PDB access code: 3IOM). RMSDs were taken after superposition against the crystallographic structure and range from 0.4 to 0.7 Å, which further validate the present docking protocol.

2.4. Virtual screening (VS)

The VS results were analyzed taking into account the piecewise linear potential (PLP), which is obtained from the MOLDOCK program.

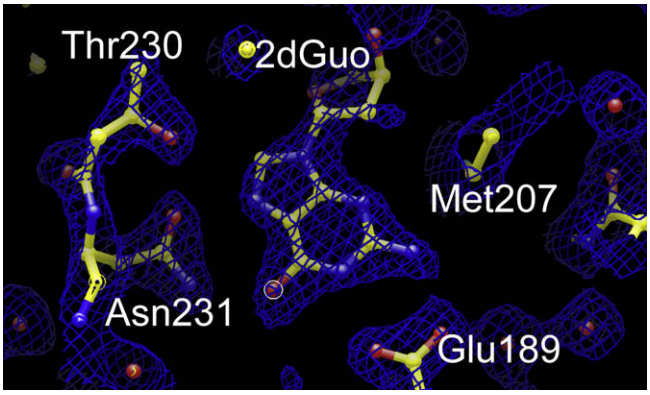

Figure 4. $2F_o - F_c$ electron density map for the active site of MtPNP contoured at 1.0 σ.

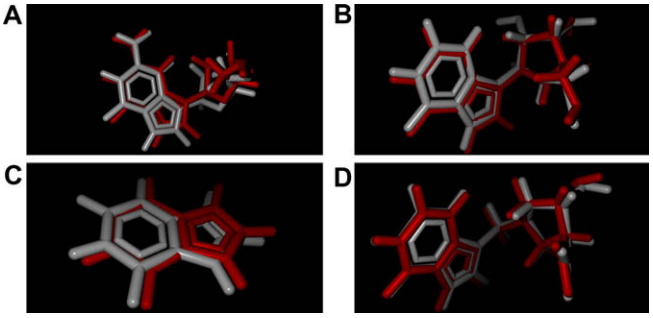

Figure 5. Crystallographic (light gray) and respective docked (dark gray) structures for complexes of MtPNP and (A) 2′-deoxyguanosine (3IOM), (B) 1,4-dideoxy-4-aza-1-(*S*)-(9-deazahypoxanthin-9-yl)-D-ribitol (1G2O), (C) 9-deazahypoxanthine (1I80), and (D) 3-hydroxy-4-hydroxymethyl-1-(4-oxo-4,4A,5,7A-tetrahydro-3*H*-pyrrolo[3,2-*d*]pyrimidin-7-ylmethyl)-pyrrolidinium (1N3I).

The small-molecule database employed in the present work was built using the purine core as inspiration. The analysis of the 581 docked structures indicated a docking re-ranking score ranging from −110.96 to 149.357, being the lowest considered the highest affinity ligand. Docking simulations of these molecules against the active site of MtPNP yielded 2-methyl-adenosine as the best ligand (lowest re-rank score: −110.96). Figure 6 shows 2-methyl-adenosine docked to the active site of MtPNP (red ligand). Analysis of the intermolecular interactions indicates the participation of Ser 36, Glu 189, Asn 231, and His 243 in intermolecular hydrogen bonds, as observed for the MtPNP:sulfate:2dGuo complex. Superposition of 2-methyl-adenosine (docking structure) with 2dGuo (crystallographic position) (white ligand) indicates that the overall intermolecular interactions are maintained with superposition of the purine rings (Fig. 6).

Especially interesting is the previously observed antimycobacterial activity of this compound. It has been reported that 2-methyl-adenosine has antimycobacterial activity that is effective in vitro and intracellularly within host macrophages.[13,27,28] Furthermore, although these previously published studies did not identify the precise mode of action for 2-methyl-adenosine, they suggested a general mode of inhibitory activity with regard to known inhibitors of RNA, DNA, and protein synthesis, which include the purine salvage pathway.

In order to further investigate protein–ligand interactions for the docked complex MtPNP and 2-methyl-adenosine, we employed a POLSCORE to estimate pK_d. We recently developed and implemented this function in the program POLSCORE,[29,30] and tested these functions against binary complexes involving PNP. Table 2

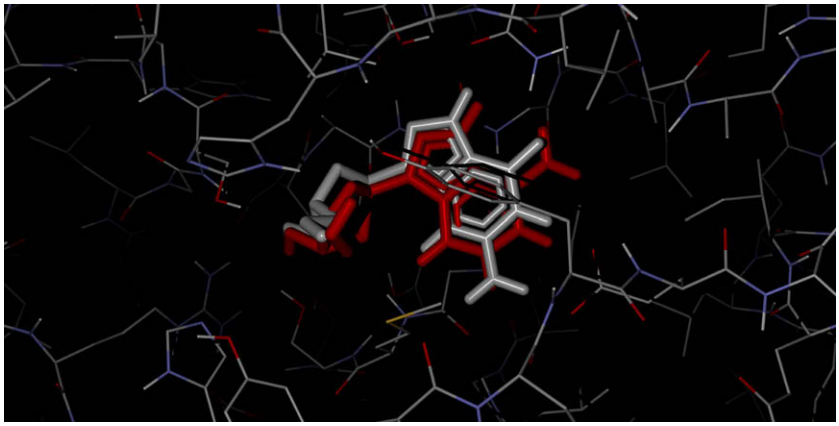

Figure 6. Structure of 2-methyl-adenosine (red) docked in the MtPNP active site and the crystallographic positioning for 2dGuo (white).

shows estimated pK_d using POLSCORE and XSCORE[38] for 10 different complexes involving HsPNP for which structural information and experimental pK_d's were available. Application of POLSCORE to this test set of 10 binary complexes generated a correlation coefficient of 0.95, against 0.58 obtained using XSCORE, which strongly indicates the ability of this computational approach to estimate binding affinity for binary complexes involving PNP. We applied this polynomial function to further evaluate binding affinity for 2-methyl-adenosine. The computational estimated K_d was 138 mM, which shows low affinity, even with the low re-rank score obtained using MOLDOCK. To confirm whether 2-methyl-adenosine inhibits MtPNP, we carried out experimental analysis of this interaction. No inhibition of MtPNP enzyme activity could be observed up to 1 mM of 2-methyl-adenosine.

These results indicate that the antimycobacterial activity of this compound cannot be attributed to MtPNP inhibition, which is in agreement with a previous report showing that MtPNP is more specific to natural 6-oxopurine nucleosides and synthetic compounds, and does not catalyze the phosphorolysis of adenosine (a 6-aminopurine nucleoside).[20] These results are also in agreement with metabolic analysis of a mutant strain of *Mycobacterium smegmatis* resistant to 2-methyl-adenosine that suggested that adenosine kinase is involved in phosphorylation of this compound to produce toxic metabolites.[39] The results here described lend support to 2-methyl-adenosine being a substrate for adenosine kinase, and to a phosphorylated form of 2-methyl-adenosine acting upon a yet unknown target in *M. tuberculosis*.

Application of POLSCORE to rank the best 100 hits identified in the docking simulations returned three transition state analogues (IMMH, DADME-IMMG, and DADME-IMMH) with pK_d ranging from 6.6 to 7.2. These compounds have been previously shown to inhibit PNP in the picomolar range.[33] 7-[[(3*R*,4*R*)-3-Hydroxy-4-(hydroxymethyl)pyrrolidin-1-yl]methyl]-1,5 dihydropyrrolo[3,2-d]pyrimidin-4-one (DADME-IMMH) had the highest pK_d, 6.6.

Our results indicate that analysis of docking solutions of PNP could be misleading, when taken alone. Additional evaluation of protein–ligand interaction employing a POLSCORE that has been shown to calculate binding affinity for PNP[29,30] improves predicting power of the present computational approach, is able to discard a false positive (2-methyl-adenosine) and, fairly important, can identify a true experimental positive result (DADME-IMMH).

3. Conclusions

The resolution of the structure of MtPNP in complex with sulfate and 2dGuo provides additional information for the structure-based design of antimycobacterial drugs, since it captures the crystal structure of an active form of the MtPNP:sulfate:2dGuo ternary complex. We employed the atomic coordinates of this structure for VS, focused on the MtPNP active site and using a database of purine analogues. In the VS simulations it was identified that 2-methyl-adenosine binds to MtPNP's active site. Previously published studies[13,27,28] reported that 2-methyl-adenosine presents antimycobacterial activity, nevertheless, without a definition of the target.

Furthermore, several purine nucleoside analogs showed selective antimycobacterial activity, 2-methyl-adenosine being the lead compound in this series, which is active against proliferating and nonproliferating bacteria due to its ability to inhibit protein synthesis.[13] The results here presented show that MtPNP is not the target of 2-methyl-adenosine inhibitory activity. In summary, analysis of the structures docked to the MtPNP active site indicates that the binding pocket has ability to accommodate molecular structures that are different from guanosine derivatives. However, our results demonstrate that caution should be exercised when

Table 2
Experimental and computational determined biding affinities for PNP complexes

Ligands[a]	pK_d (experimental)[45]	pK_d (POLSCORE)[29,30]	pK_d (XSCORE)[38]
Allopurinol (1,2-dihydropyrazolo[3,4-*d*]pyrimidin-4-one)	3.0	2.3	4.5
Quinazolinone (1*H*-quinazolin-4-one)	3.5	3.5	5.2
Oxoallopurinol (1,2-dihydropyrazolo[3,4-*d*]pyrimidine-4,6-dione)	3.1	2.8	4.7
Methylthioinosine (2-(hydroxymethyl)-5-(6-methylsulfanylpurin-9-yl)oxolane-3,4-diol)	4.9	5.3	5.5
Acyclovir (2-amino-9-(2-hydroxyethoxymethyl)-3*H*-purin-6-one)	4.9	4.5	5.0
6-Mercaptopurine (3,7-dihydropurine-6-thione)	4.1	3.6	4.6
5-Chloro-5-deoxy-8-aminoguanosine (5-chloro-2-amino-9-[(2*R*,3*R*,4*S*,5*R*)-3-amino-4-hydroxy-5-(hydroxymethyl)oxolan-2-yl]-3*H*-purin-6-one)	6.4	5.7	5.4
2-Amino-6-methylthiopurine (6-methylsulfanyl-7*H*-purin-2-amine)	3.5	3.5	4.9
Ganciclovir (2-amino-9-(1,3-dihydroxypropan-2-yloxymethyl)-3*H*-purin-6-one)	4.8	4.8	4.5
9-Benzylguanine (6-phenylmethoxy-7*H*-purin-2-amine)	5.3	5.2	5.2

[a] IUPAC names indicated in parenthesis.

trying to select enzyme activity inhibitors only by molecular docking simulations. Application of additional computational analysis using POLSCORE was able to furnish more reliable information, confirmed by experimental analysis of protein–ligand interaction. It seems that application of POLSCORE to rank molecular docking results, obtained with MOLDOCK, is able to eliminate false positives and also to identify PNP inhibitors, as DADME-IMMH, that presented the highest pK_d in the data set of 581 molecules, with better overall performance than the native MOLDOCK scoring functions.

As compared with the standard MOLDOCK scoring functions (MOLDOCK Score and re-ranking Score), the new ranking criterion employing polynomial empirical scoring function implemented in the program POLSCORE considerably improved the selection of correct docking solutions tested here, which opens the possibility to scan vast small-molecule libraries employing a more reliable scoring function to predict binding affinity.

4. Experimental

All chemicals used were of analytical or reagent grade and required no further purification. Na_2SO_4 and $MgCl_2$ were from Merck, 2dGuo and poly(ethylene glycol) 3350 were from Fluka BioChemika, Tris was from Acros, MESG is commercially available in the Enzchek phosphate assay kit from Molecular Probes, and 2-methyladenosine was a generous gift of Professor William B. Parker.

4.1. Crystallization, data collection and processing

Recombinant MtPNP was expressed and purified as previously described.[20] The protein was cocrystallized in a 2:0.5:1 stoichiometry with Na_2SO_4 (500 mM) and 2dGuo (3 mM), respectively, by hanging-drop vapor diffusion at 18 °C. MtPNP protein [1 μL of 25 mg mL^{-1} in Tris pH 7.6 (50 mM)] had been previously mixed with an equal volume of the reservoir solution containing Tris pH 8.0 (100 mM), poly(ethylene glycol) 3350 (25%), and $MgCl_2$ (25 mM), and hanging drops (3.5 μL) were equilibrated against the reservoir solution (400 μL). Diffraction from the crystals was consistent with the space group H3 ($a = b = 113.48$ Å, $c = 85.01$ Å), with a dimer in the asymmetric unit.

MtPNP:sulfate:2dGuo crystals were cryoprotected by transfer to crystallization solution supplemented with glycerol (50%) and flash-cooled at 100 K. X-ray diffraction data were collected at 1.428 Å wavelength on a CDD detector (MARCCD) using synchrotron radiation at beamline D03B-MX1 at the Synchrotron Radiation Source (Laboratório Nacional de Luz Síncrotron—LNLS, Campinas, SP, Brazil) with an exposure time of 60 s per image at a distance from crystal to detector of 80 mm. X-ray diffraction data were processed to 2.15 Å resolution using the program MOSFLM and scaled with the program SCALA.[40] The data set for MtPNP:sulfate:2dGuo was 96.9% complete to 2.15 Å resolution with R_{sym} of 8.6%. In the highest resolution shell (2.27–2.15 Å), the reflections presented R_{sym} of 13.8%.

4.2. Structure resolution and refinement

The crystal structure of MtPNP:sulfate:2dGuo was solved by standard molecular replacement methods using AMoRe software package,[41] incorporated in the CCP4 program package,[40] with MtPNP (PDB Accession No. 1G2O)[26] as the search model; the ligand and water molecules were removed from the model. The best solution after rigid-body refinement yielded an initial R_{factor} of 28% and a correlation coefficient of 76% using data in the resolution range of 8–3 Å. We performed structure refinement using REFMAC,[40] and atomic positions obtained from molecular replacement were used to initiate the crystallographic refinement. The overall stereochemistry quality of the final structure for MtPNP:sulfate:2dGuo ternary complex was assessed by the program PARMODEL.[42] The trimeric structure and atomic models were superposed using the program LSQKAB from CCP4.[40]

4.3. Molecular docking

Docking applications can be classified by their search algorithm, which is defined by a set of rules and parameters applied to predict the conformations. When we consider the flexibility of the ligand and/or the receptor docking, algorithms can be classified into two major groups: rigid-body and flexible docking. We applied the flexible docking protocol available in the program MOLDOCK,[36,37] where the flexibility of the ligand is simulated. MOLDOCK is an implementation of a heuristic search algorithm that joins together differential evolution with a cavity calculation algorithm. In addition, MOLDOCK evaluates the best poses applying a docking scoring function, which uses PLP, previously implemented in the program GEMDOCK.[43,44] In the program MOLDOCK, the docking scoring function is extended with an additional term, taking hydrogen bonds directionality into account. In addition a re-ranking procedure is also applied in order to augment docking accuracy.

In order to validate the present docking protocol we performed the docking simulation against the active site of MtPNP and compared with the crystallographic structures. We used the default protocol of MOLDOCK with center at coordinates $x = 50.57$, $y = -49.23$, and $z = 24.07$ Å, and docking sphere with radius of 15 Å. Figure 7 shows the docking sphere used in the re-docking simulations. The cavity search algorithm was set to identify up to 10 cavities in the structure. Sulfate molecules identified in the crystallographic structure were kept in the structure of the dimer identified in the asymmetric unit during the docking simulations. All simulations were performed in an iMac (Intel Processor Core 2 Duo, 2.66 GHz, 2 GB SDRAM DDR3 1066 MHz).

It has been proposed that purine nucleoside is an important pharmacophore for the development of antimycobacterial drugs.[13,45] The pharmacophore is an effort to capture the main structural aspects of the protein–ligand interaction. Therefore, it has to be specific enough to be functional for a particular target and, at the same time, general enough so that the information can be employed to find new molecules that are likely to bind the target. Based on this observation, we employed the purine core to carry out a search in the ZINC database[46] to build a small-molecule database, using the pharmacophoric fingerprints of purine with a Tanimoto coefficient cutoff of 60%. A total of 581 molecules were retrieved and used to build this database (Supplementary

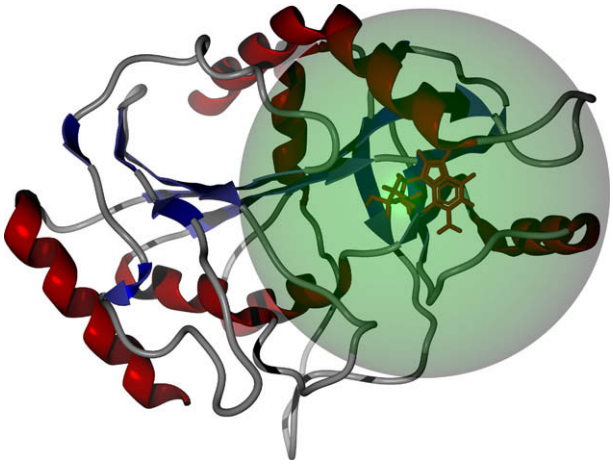

Figure 7. Docking sphere used in the re-docking and virtual screening simulations. This sphere has a radius of 15 Å and it is centered at the active site of MtPNP.

data), which is also available for download at http://azevedolab.net.[47] To perform molecular docking simulations, we employed the validated protocol described above.

Protein–ligand interactions were further investigated by use of polynomial empirical scoring functions implemented in the program POLSCORE.[29,30] This polynomial function is shown below:

$$pK_d = c_0 + c_1HB + c_2HB^2 + c_3HC + c_4HB * HC + c_5HC^2 + c_6RT + c_7VDW$$

where c_j are weighting terms for each term present in the scoring function. Multivariate regression analysis was applied to find the best fit between the predicted and experimental protein-binding affinities obtained from a training set with crystallographic structures for which experimental binding information is available. HB is the intermolecular hydrogen bond terms, HC is the intermolecular hydrophobic contact, RT is the deformation effect, VDW describes van der Waals and pK_d is $-\log K_d$, and the latter represents the overall dissociation constant for binary complex formation. All these terms have been incorporated in the program POLSCORE, previously described by our group.[29,30] POLSCORE function was integrated in a protocol to rank docking solutions obtained with MOLDOCK.

We also employed a validated empirical scoring function implemented in the program XSCORE[38] to compare with POLSCORE. We applied both methodologies to a test set of 10 binary complexes involving HsPNP for which structural and binding information is available.

4.4. MtPNP enzyme activity assays

2-Methyl-adenosine was solubilized in dimethyl sulfoxide (DMSO). MtPNP enzyme activity assays were carried out under initial rate conditions at 25 °C in 100 mM *N*-2-hydroxyethylpiperazine-*N*′-2-ethanesulfonic acid (HEPES) pH 7.0 (500 μL total reaction volume). The MtPNP conversion of 2-amino-6-mercapto-7-methylpurine from MESG (ε = 11,000 M^{-1} cm^{-1} at 360 nm) was monitored spectrophotometrically by the change in absorbance in the presence of inorganic phosphate. MESG and inorganic phosphate concentrations were maintained close to their K_M values[20] in either absence or presence of 2-methyl-adenosine in the reaction mixture to evaluate any possible inhibitory effect.

4.5. Deposit

The atomic coordinates and structure factors for the MtPNP:sulfate:2dGuo structure have been deposited at the Protein Data Bank, access code: 3IOM.

Acknowledgements

This work was supported by Millennium Initiative Program and National Institute of Science and Technology in Tuberculosis (INCT-TB), MCT-CNPq, Ministry of Health—Department of Science and Technology (DECIT)—Secretary of Health Policy (Brazil) to L.A.B., D.S.S., and W.F.A Jr. L.A.B. (CNPq, 520182/99-5), D.S.S. (CNPq, 304051/1975-06), and W.F.A. Jr are Research Career Awardees of the National Research Council of Brazil (CNPq). R.G.D. is a postdoctoral fellow of CNPq. We thank Professor William B. Parker, Southern Research Institute, Birminghan, and Department of Pharmacology and Toxicology, University of Alabama at Birmingham, for his generous gift of 2-methyl-adenosine.

Supplementary data

Supplementary data associated with this article can be found, in the online version, at doi:10.1016/j.bmc.2010.05.009.

References and notes

1. Enarson, D. A.; Murray, J. F. In *Tuberculosis*; Rom, W. M., Garay, S., Eds.; Little Brown and Co.: Boston, 1996; pp 57–75.
2. World Health Organization, Global Tuberculosis Control, WHO Report, 1998.
3. World Health Organization, Global Tuberculosis Control, WHO Report, 2004.
4. Young, D. B. *Nature* **1998**, *393*, 515.
5. Bloom, B. R.; Murray, C. J. L. *Science* **1992**, *257*, 1055.
6. World Health Organization Global tuberculosis programme—Tuberculosis Fact Sheet, 1998.
7. World Health Organization. *Saudi Med. J.* **2004**, *25*, 1139.
8. Petrini, B.; Hoffner, S. *Int. J. Antimicrob. Agents* **1999**, *13*, 93.
9. Colditz, G. A.; Brewer, T. F.; Berkey, C. S.; Wilson, M. E.; Burdick, E.; Fineberg, H. V.; Mosteller, F. *J. Am. Med. Assoc.* **1994**, *271*, 698.
10. Ducati, R. G.; Ruffino-Netto, A.; Basso, L. A.; Santos, D. S. *Mem. Inst. Oswaldo Cruz* **2006**, *101*, 697.
11. Cole, S. T.; Brosch, R.; Parkhill, J.; Garnier, T.; Churcher, C.; Harris, D.; Gordon, S. V.; Eiglmeier, K.; Gas, S.; Barry, C. E., III; Tekaia, F.; Badcock, K.; Basham, D.; Brown, D.; Chillingworth, T.; Connor, R.; Davies, R.; Devlin, K.; Feltwell, T.; Gentles, S.; Hamlin, N.; Holroyd, S.; Hornsby, T.; Jagels, K.; Barrel, B. G. *Nature* **1998**, *393*, 537.
12. Ducati, R. G.; Basso, L. A.; Santos, D. S. *Curr. Drug Targets* **2007**, *8*, 423.
13. Parker, W. B.; Long, M. C. *Curr. Pharm. Des.* **2007**, *13*, 599.
14. Kalckar, H. M. *J. Biol. Chem.* **1947**, *167*, 429.
15. Ojha, A. K.; Mukherjee, T. K.; Chatterji, D. *Infect. Immun.* **2000**, *68*, 4084.
16. Primm, T. P.; Andersen, S. J.; Mizrahi, V.; Avarbock, D.; Rubin, H.; Barry, C. E., III *J. Bacteriol.* **2000**, *182*, 4889.
17. Bzowska, A.; Kulikowska, E.; Shugar, D. *Pharmacol. Ther.* **2000**, *88*, 349.
18. Mao, C.; Cook, W. J.; Zhou, M.; Koszalka, G. W.; Krenitsky, T. A.; Ealick, S. E. *Structure* **1997**, *5*, 1373.
19. Taylor Ringia, E. A.; Tyler, P. C.; Evans, G. B.; Furneaux, R. H.; Murkin, A. S.; Schramm, V. L. *J. Am. Chem. Soc.* **2006**, *128*, 7126.
20. Ducati, R. G.; Santos, D. S.; Basso, L. A. *Arch. Biochem. Biophys.* **2009**, *486*, 155.
21. Bzowska, A.; Kulikowska, E.; Shugar, D. *Z. Naturforsch.* **1990**, *45*, 59.
22. Jensen, K. F. *Eur. J. Biochem.* **1976**, *61*, 377.
23. Tebbe, J.; Bzowska, A.; Wielgus-Kutrowska, B.; Schröder, W.; Kazimierczuk, Z.; Shugar, D.; Saenger, W.; Koellner, G. *J. Mol. Biol.* **1999**, *294*, 1239.
24. Tahirov, T. H.; Inagaki, E.; Ohshima, N.; Kitao, T.; Kuroishi, C.; Ukita, Y.; Takio, K.; Kobayashi, M.; Kuramitsu, S.; Yokoyama, S.; Miyano, M. *J. Mol. Biol.* **2004**, *337*, 1149.
25. Basso, L. A.; Santos, D. S.; Shi, W.; Furneaux, R. H.; Tyler, P. C.; Schramm, V. L.; Blanchard, J. S. *Biochemistry* **2001**, *40*, 8196.
26. Shi, W.; Basso, L. A.; Santos, D. S.; Tyler, P. C.; Furneaux, R. H.; Blanchard, J. S.; Almo, S. C.; Schramm, V. L. *Biochemistry* **2001**, *40*, 8204.
27. Barrow, E. W.; Westbrook, L.; Bansal, N.; Suling, W. J.; Maddry, J. A.; Parker, W. B.; Barrow, W. W. *J. Antimicrob. Chemother.* **2003**, *52*, 801.
28. Parker, W. B.; Barrow, E. W.; Allan, P. W.; Shaddix, S. C.; Long, M. C.; Barrow, W. W.; Bansal, N.; Maddry, J. A. *Tuberculosis (Edinb)* **2004**, *84*, 327.
29. De Azevedo, W. F., Jr.; Dias, R. *Bioorg. Med. Chem.* **2008**, *16*, 9378.
30. Dias, R.; Timmers, L. F.; Caceres, R. A.; de Azevedo, W. F., Jr. *Curr. Drug Targets* **2008**, *9*, 1062.
31. Silva, R. G.; Pereira, J. H.; Canduri, F.; de Azevedo, W. F., Jr.; Basso, L. A.; Santos, D. S. *Arch. Biochem. Biophys.* **2005**, *442*, 49.
32. Nolasco, D. O.; Canduri, F.; Pereira, J. H.; Cortinóz, J. R.; Palma, M. S.; Oliveira, J. S.; Basso, L. A.; de Azevedo, W. F., Jr.; Santos, D. S. *Biochem. Biophys. Res. Commun.* **2004**, *324*, 789.
33. Lewandowicz, A.; Shi, W.; Evans, G. B.; Tyler, P. C.; Furneaux, R. H.; Basso, L. A.; Santos, D. S.; Almo, S. C.; Schramm, V. L. *Biochemistry* **2003**, *42*, 6057.
34. De Azevedo, W. F., Jr.; Mueller-Dieckmann, H. J.; Schulze-Gahmen, U.; Worland, P. J.; Sausville, E.; Kim, S. H. *Proc. Natl. Acad. Sci. U.S.A.* **1996**, *93*, 2735.
35. De Azevedo, W. F.; Leclerc, S.; Meijer, L.; Havlicek, L.; Strnad, M.; Kim, S. H. *Eur. J. Biochem.* **1997**, *243*, 518.
36. Thomsen, R.; Christensen, M. H. *J. Med. Chem.* **2006**, *49*, 3315.
37. De Azevedo, W. F., Jr. *Curr. Drug Targets* **2010**, *11*, 327.
38. Wang, R.; Lai, L.; Wang, S. *J. Comput. Aided Mol. Des.* **2002**, *16*, 11.
39. Chen, C. K.; Barrow, E. W.; Allan, P. W.; Bansal, N.; Maddry, J. A.; Suling, W. J.; Parker, W. B. *Microbiology* **2002**, *148*, 289.
40. Collaborative Computational Project, Number 4 *Acta Crystallogr., Sect. D* **1994**, *50*, 760.
41. Navaza, J. *Acta Crystallogr., Sect. A* **1994**, *50*, 157.
42. Uchôa, H. B.; Jorge, G. E.; Freitas da Silveira, N. J.; Camera, J. C., Jr.; Canduri, F.; de Azevedo, W. F., Jr. *Biochem. Biophys. Res. Commun.* **2004**, *325*, 1481.
43. De Azevedo, W. F., Jr. *Curr. Drug Targets* **2010**, *11*, 261.
44. Yang, J.-M.; Chen, C.-C. *Proteins* **2004**, *55*, 288.
45. Timmers, L. F.; Caceres, R. A.; Vivan, A. L.; Gava, L. M.; Dias, R.; Ducati, R. G.; Basso, L. A.; Santos, D. S.; de Azevedo, W. F., Jr. *Arch. Biochem. Biophys.* **2008**, *479*, 28.
46. Irwin, J. J.; Shoichet, B. K. *J. Chem. Inf. Model.* **2005**, *45*, 177.
47. Timmers, L. F.; Pauli, I.; Caceres, R. A.; de Azevedo, W. F., Jr. *Curr. Drug Targets* **2008**, *9*, 1092.